



## COPY RIGHT

**2018 IJIEMR.** Personal use of this material is permitted. Permission from IJIEMR must be obtained for all other uses, in any current or future media, including reprinting/republishing this material for advertising or promotional purposes, creating new collective works, for resale or redistribution to servers or lists, or reuse of any copyrighted component of this work in other works. No Reprint should be done to this paper, all copy right is authenticated to Paper Authors

IJIEMR Transactions, online available on 3<sup>rd</sup> March 2018. Link :

<http://www.ijiemr.org/downloads.php?vol=Volume-7&issue=ISSUE-03>

Title: Solar PV Array-Fed Water Pumping System Using Zeta Converter based Closed-Loop Control of BLDC Motor Drive.

Volume 07, Issue 03, Page No: 1-10

Paper Authors

**\*B. VEERABABU, A.S.S. VEERENDRABABU.**

\* Dept of EEE, Aditya College of Engineering.



USE THIS BARCODE TO ACCESS YOUR ONLINE PAPER

To Secure Your Paper As Per **UGC Guidelines** We Are Providing A Electronic Bar Code

## SOLAR PV ARRAY-FED WATER PUMPING SYSTEM USING ZETA CONVERTER BASED CLOSED-LOOP CONTROL OF BLDC MOTOR DRIVE

\*B. VEERABABU, \*\*A.S.S. VEERENDRABABU

\*PG Scholar, Dept of EEE, Aditya College of Engineering, Surampalem, E.g (Dt), Andhrapradesh, India.

\*\*Assistant Professor, Dept of EEE, Aditya College of Engineering, Surampalem, E.g (Dt), Andhrapradesh, India.

[arigelaveerendra@gmail.com](mailto:arigelaveerendra@gmail.com) [einstein.veera@gmail.com](mailto:einstein.veera@gmail.com)

### ABSTRACT:

This paper proposes a solar photovoltaic (SPV) array fed water pumping system utilizing a zeta converter as an intermediate DC-DC converter in order to extract the maximum available power from the SPV array. Controlling the zeta converter in an intelligent manner through the incremental conductance maximum power point tracking (INC-MPPT) algorithm offers the soft starting of the brushless DC (BLDC) motor employed to drive a centrifugal water pump coupled to its shaft. Soft starting i.e. the reduced current starting inhibits the harmful effect of the high starting current on the windings of the BLDC motor. A fundamental frequency switching of the voltage source inverter (VSI) is accomplished by the electronic commutation of the BLDC motor, thereby avoiding the VSI losses occurred owing to the high frequency switching. A new design approach for the low valued DC link capacitor of VSI is proposed. The proposed water pumping system is designed and modeled such that the performance is not affected even under the dynamic conditions. Suitability of the proposed system under dynamic conditions is demonstrated by the simulation results using MATLAB/Simulink software.

**Key words:** Brushless dc (BLDC) motor, incremental conductance maximum power point tracking (INC-MPPT), solar photovoltaic (SPV) array, voltage-source inverter (VSI), water pump, zeta converter

### I. INTRODUCTION

Severe environmental protection regulations, shortage of fossil fuels and eternal energy from the sun have motivated these researchers towards the solar photovoltaic (SPV) array generated electrical power for various applications [1]. Water pumping is receiving wide attention nowadays amongst all the applications of SPV array. To enhance the efficiency of SPV array and hence the whole system regardless of the operating conditions, it becomes essential to operate SPV array at its maximum power point by means of a maximum power point tracking (MPPT) algorithm [2-4]. Various DC-DC converters have been already employed to accomplish this action of MPPT. Nevertheless, a Zeta converter [5 -9] based MPPT is still unexplored in any kind of SPV array based applications. An incremental conductance (INC) MPPT algorithm [2] is used

in this work in order to generate an optimum value of duty cycle for the IGBT (Insulated Gate Bipolar Transistor) switch of Zeta converter such that the SPV array is constrained to operate at its MPP. Various configurations of Zeta converters such as self-lift circuit, re-lift circuit, triple-lift circuit and quadruple-lift circuit using voltage lift (VL) technique have been reported in aforementioned topologies have high voltage transfer gain but at the cost of increased number of components and switching devices. Therefore, these topologies of Zeta converter do not suit the proposed water pumping system.

The PV inverters dedicated to the small PV plants must be characterized by a large range for the input voltage in order to accept different configurations of the PV field. This capability is assured by adopting inverters based on a double stage architecture where the

first stage, which usually is a dc/dc converter, can be used to adapt the PV array voltage in order to meet the requirements of the dc/ac second stage, which is used to supply an ac load or to inject the produced power into the grid. This configuration is effective also in terms of controllability because the first stage can be devoted to track the maximum power from the PV array, while the second stage is used to produce ac current with low Total Harmonic Distortion (THD).

BLDC motors are preferred over DC motors and induction motors due to their advantages like long operating life, higher efficiency, low maintenance and better speed torque characteristics. Stator windings of BLDC motors are energized in a sequence from an inverter. A bulkier DC link capacitor is connected in between the dc-dc converter and inverter to get a constant voltage at the input of inverter, thus to make the voltage ripple free. But the DC link capacitor is bulkier in size and its life time is affected by operating temperature. Moreover the cost is about 5-15% of overall cost of BLDC motor drive. As an attempt to reduce the cost of motor, DC link capacitor can be eliminated at the expense of torque ripple. Thus a new torque ripple compensation technique is proposed to compensate for the torque ripple associated with the elimination of the DC link capacitor. In this method, torque ripple compensation technique is proposed to a solar PV array fed DC link capacitor free BLDC motor.

The permanent magnet brushless DC (BLDC) motor is employed to drive a centrifugal water pump coupled to its shaft. The BLDC motor is selected because of its merits [7,9] useful for the development of suitable water pumping system. This electronically commutated BLDC motor [9-11] is supplied by a voltage source inverter (VSI) which is operated by fundamental frequency switching

resulting in low switching losses [12-15]. Suitability of the proposed SPV array fed water pumping system subjected to various operating and environmental conditions is demonstrated by satisfactory simulated results using MATLAB/Simulink environment.

The existing literature exploring SPV array-based BLDC motor-driven water pump is based on a configuration shown in Fig.1. A dc-dc converter is used for MPPT of an SPV array as usual. Two phase currents are sensed along with Hall signals feedback for control of BLDC motor, resulting in an increased cost. The additional control scheme causes increased cost and complexity, which is required to control the speed of BLDC motor. Moreover, usually a voltage-source inverter (VSI) is operated with high-frequency PWM pulses, resulting in an increased switching loss and hence the reduced efficiency.

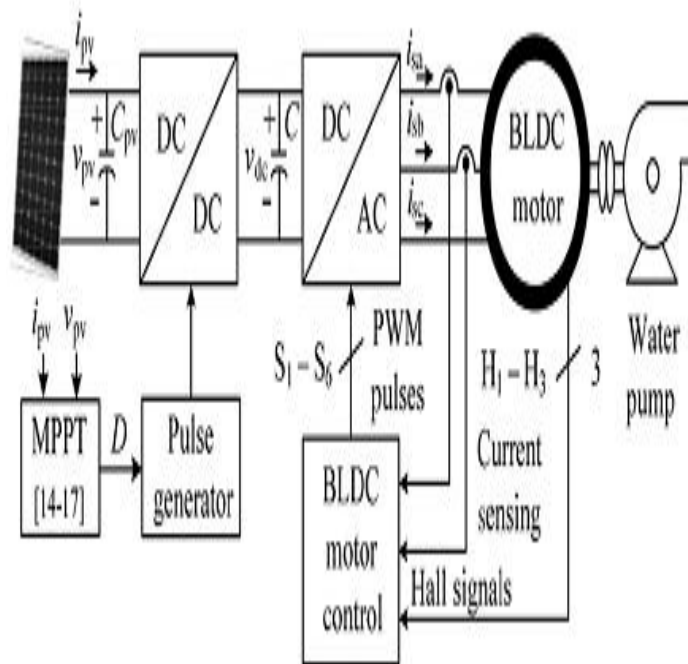


Fig.1. Conventional SPV-fed BLDC motor-driven water pumping system

## II. CONFIGURATION OF PROPOSED SYSTEM

The structure of proposed SPV array-fed BLDC motordriven water pumping system employing a zeta converter is shown in Fig.3.2. The proposed system consists of (left to right) an SPV array, a zeta converter, a VSI, a BLDC motor, and a water pump. The BLDC motor has an inbuilt encoder. The pulse generator is used to operate the zeta converter. A step-by-step operation of proposed system is elaborated in Section III in detail.

## III. OPERATION OF PROPOSED SYSTEM

The SPV array generates the electrical power demanded by the motor-pump. This electrical power is fed to the motor-pump via a zeta converter and a VSI. The SPV array appears as a power source for the zeta converter as shown in Fig.2. Ideally, the same amount of power is transferred at the output of zeta converter which appears as an input source for the VSI. In practice, due to the various losses associated with a dc-dc converter [23], slightly less amount of power is transferred to feed the VSI. The pulse generator generates, through INCMPPT algorithm, switching pulses for insulated gate bipolar transistor (IGBT) switch of the zeta converter. The INC-MPPT algorithm uses voltage and current as feedback from SPV array and generates an optimum value of duty cycle. Further, it generates actual switching pulse by comparing the duty cycle with a high-frequency carrier wave. In this way, the maximum power extraction and hence the efficiency optimization of the SPV array is accomplished.

The VSI, converting dc output from a zeta converter into ac, feeds the BLDC motor to drive a water pump coupled to its shaft. The VSI is operated in fundamental frequency switching through an electronic commutation of BLDC motor assisted by its built-in encoder.

The high frequency switching losses are thereby eliminated, contributing in an increased efficiency of proposed water pumping system.

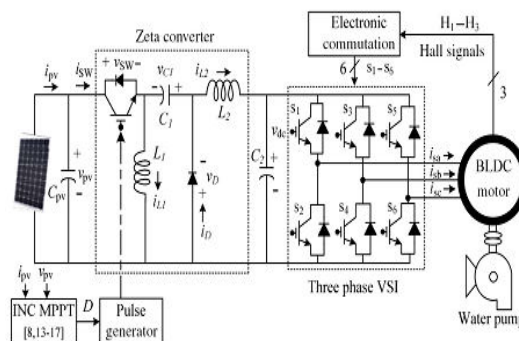


Fig.2. Proposed SPV-zeta converter-fed BLDC motor drive for water pump

## IV. DESIGN OF PROPOSED SYSTEM

Various operating stages shown in Fig.2 are properly designed to develop an effective water pumping system, capable of operating under uncertain conditions. A BLDC motor of 2.89-kW power rating and an SPV array of 3.4-kW peak power capacity under standard test conditions (STC) are selected to design the proposed system. The detailed designs of various stages such as SPV array, zeta converter, and water pump are described as follows.

### A. Design of SPV Array

As per above discussion, the practical converters are associated with various power losses. In addition, the performance of BLDC motor-pump is influenced by associated mechanical and electrical losses. To compensate these losses, the size of SPV array is selected with slightly more peak power capacity to ensure the satisfactory operation regardless of power losses. Therefore, the SPV array of peak power capacity of  $P_{mpp}=3.4$  kW under STC (STC:  $1000$  W/m<sup>2</sup>,  $25^{\circ}$ C, AM 1.5), slightly more than demanded by the motor-pump is selected and its parameters are designed accordingly. SolarWorld make Sunmodule Plus

SW 280 mono [24] SPV module is selected to design the SPV array of an appropriate size. Electrical specifications of this module are listed in Table 3.1 and numbers of modules required to connect in series/parallel are estimated by selecting the voltage of SPV array at MPP under STC as  $V_{mpp} = 187.2V$ .

**TABLE 1**  
Specifications of Sun module plus SW 280 mono SPV Module

Peak power, $P_m$ (W)	280
Open circuit voltage, $V_o$ (V)	39.5
Voltage at MPP, $V_m$ (V)	31.2
Short circuit current, $I_s$ (A)	9.71
Current at MPP, $I_m$ (A)	9.07
Number of cells connected in series, $N_{sc}$	60

The current of SPV array at MPP  $I_{mpp}$  is estimated as

$$I_{mpp} = P_{mpp}/V_{mpp} = 3400/187.2 = 18.16 \text{ A} \quad (1)$$

The numbers of modules required to connect in series are as follows:

$$N_s = V_{mpp}/V_m = 187.2/31.2 = 6. \quad (2)$$

The numbers of modules required to connect in parallel areas follows:

$$N_p = I_{mpp}/I_m = 18.16/9.07 = 2. \quad (3)$$

Connecting six modules in series, having two strings in parallel, an SPV array of required size is designed for the proposed system.

## B. Design of Zeta Converter

The zeta converter is the next stage to the SPV array. Its design consists of an estimation of various components such as input inductor  $L_1$ , output inductor  $L_2$ , and intermediate capacitor  $C_1$ . These components are designed such that the zeta converter always

operates in CCM resulting in reduced stress on its components and devices. An estimation of the duty cycle  $D$  initiates the design of zeta converter which is estimated as [6]

$$D = \frac{V_{dc}}{V_{dc} + V_{mpp}} = \frac{200}{200 + 187.2} = 0.52 \quad (4)$$

Where  $V_{dc}$  is an average value of output voltage of the zeta converter (dc link voltage of VSI) equal to the dc voltage rating of the BLDC motor.

An average current flowing through the dc link of the VSI  $I_{dc}$  is estimated as

$$I_{dc} = P_{mpp}/V_{dc} = 3400/200 = 17 \text{ A}. \quad (5)$$

Then,  $L_1$ ,  $L_2$ , and  $C_1$  are estimated as

$$L_1 = \frac{DV_{mpp}}{f_{sw}\Delta I_{L1}} = \frac{0.52 \times 187.2}{20000 \times 18.16 \times 0.06} = 4.5 \times 10^{-3} \approx 5 \text{ mH} \quad (6)$$

$$L_2 = \frac{(1-D)V_{dc}}{f_{sw}\Delta I_{L2}} = \frac{(1-0.52) \times 200}{20000 \times 17 \times 0.06} = 4.7 \times 10^{-3} \approx 5 \text{ mH} \quad (7)$$

$$C_1 = \frac{DI_{dc}}{f_{sw}\Delta V_{C1}} = \frac{0.52 \times 17}{20000 \times 200 \times 0.1} = 22 \mu\text{F} \quad (8)$$

Where  $f_{sw}$  is the switching frequency of IGBT switch of the zeta converter;  $\Delta I_{L1}$  is the amount of permitted ripple in the current flowing through  $L_1$ , same as  $I_{L1} = I_{mpp}$ ;  $\Delta I_{L2}$  is the amount of permitted ripple in the current flowing through  $L_2$ , same as  $I_{L2} = I_{dc}$ ;  $\Delta V_{C1}$  is the permitted ripple in the voltage across  $C_1$ , same as  $V_{C1} = V_{dc}$ .

## C. Estimation of DC-Link Capacitor of VSI

A new design approach for estimation of dc-link capacitor of the VSI is presented here. This approach is based on a fact that sixth harmonic component of the supply (ac) voltage is reflected on the dc side as a dominant harmonic in the three-phase supply system [25].

Here, the fundamental frequencies of output voltage of the VSI are estimated corresponding to the rated speed and the minimum speed of BLDC motor essentially required pumping the water. These two frequencies are further used to estimate the values of their corresponding capacitors. Out of these two estimated capacitors, larger one is selected to assure a satisfactory operation of proposed system even under the minimum solar irradiance level.

The fundamental output frequency of VSI corresponding to the rated speed of BLDC motor  $\omega_{rated}$  is estimated as

$$\omega_{rated} = 2\pi f_{rated} = 2\pi \frac{N_{rated} P}{120} = 2\pi \times \frac{3000 \times 6}{120} = 942 \text{ rad/s.} \quad (9)$$

The fundamental output frequency of the VSI corresponding to the minimum speed of the BLDC motor essentially required to pump the water ( $N = 1100 \text{ r/min}$ )  $\omega_{min}$  is estimated as

$$\omega_{min} = 2\pi f_{min} = 2\pi \frac{NP}{120} = 2\pi \times \frac{1100 \times 6}{120} = 345.57 \text{ rad/s} \quad (10)$$

Where  $f_{rated}$  and  $f_{min}$  are fundamental frequencies of output voltage of VSI corresponding to a rated speed and a minimum speed of BLDC motor essentially required to pump the water, respectively, in Hz;  $N_{rated}$  is rated speed of the BLDC motor;  $P$  is a number of poles in the BLDC motor.

The value of dc link capacitor of VSI at  $\omega_{rated}$  is as follows:

$$C_{2,rated} = \frac{I_{dc}}{6 \times \omega_{rated} \times \Delta V_{dc}} = \frac{17}{6 \times 942 \times 200 \times 0.1} = 150.4 \mu\text{F.} \quad (11)$$

Similarly, a value of dc link capacitor of VSI at  $\omega_{min}$  is as follows:

$$C_{2,min} = \frac{I_{dc}}{6 \times \omega_{min} \times \Delta V_{dc}} = \frac{17}{6 \times 345.57 \times 200 \times 0.1} = 410 \mu\text{F} \quad (12)$$

Where  $\Delta V_{dc}$  is an amount of permitted ripple in voltage across dc-link

capacitor  $C_2$ . Finally,  $C_2 = 410 \mu\text{F}$  is selected to design the dc-link capacitor.

## D Design of Water Pump

To estimate the proportionality constant  $K$  for the selected water pump, its power-speed characteristics [26], [27] is used as

$$K = \frac{P}{\omega_r^3} = \frac{2.89 \times 10^3}{(2\pi \times 3000/60)^3} = 9.32 \times 10^{-5} \quad (13)$$

Where  $P = 2.89 \text{ kW}$  is rated power developed by the BLDC motor and  $\omega_r$  is rated mechanical speed of the rotor (3000 r/min) in rad/s.

A water pump with these data is selected for proposed system.

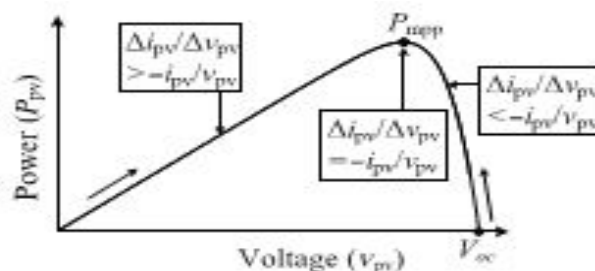


Fig.3. Illustration of INC-MPPT with SPV array  $P_{pv}-v_{pv}$  characteristics.

TABLE.2

Switching States for Electronic Commutation of BLDC Motor

Rotor position $\theta$ (°)	Hall signals			Switching states					
	$H_3$	$H_2$	$H_1$	$S_1$	$S_2$	$S_3$	$S_4$	$S_5$	$S_6$
NA	0	0	0	0	0	0	0	0	0
0-60	1	0	1	1	0	0	1	0	0
60-120	0	0	1	1	0	0	0	0	1
120-180	0	1	1	0	0	1	0	0	1
180-240	0	1	0	0	1	1	0	0	0
240-300	1	1	0	0	1	0	0	1	0
300-360	1	0	0	0	0	0	1	1	0
NA	1	1	1	0	0	0	0	0	0

## V. CONTROL OF PROPOSED SYSTEM

The proposed system is controlled in two stages. These two control techniques, viz., MPPT and electronic commutation, are discussed as follows.

## A. INC-MPPT Algorithm

An efficient and commonly used INC-MPPT technique [8],[13] in various SPV array based applications is utilized in order to optimize the power available from a SPV array and to facilitate a soft starting of BLDC motor. This technique allows perturbation in either the SPV array voltage or the duty cycle. The former calls for a proportional-integral (PI) controller to generate a duty cycle [8] for the zeta converter, which increases the complexity. Hence, the direct duty cycle control is adapted in this work. The INC-MPPT algorithm determines the direction of perturbation based on the slope of  $P_{pv}-v_{pv}$  curve, shown in Fig.3. As shown in Fig.3, the slope is zero at MPP, positive on the left, and negative on the right of MPP, i.e.,

$$\left. \begin{aligned} \frac{dP_{pv}}{dv_{pv}} &= 0; && \text{at mpp} \\ \frac{dP_{pv}}{dv_{pv}} &> 0; && \text{left of mpp} \\ \frac{dP_{pv}}{dv_{pv}} &< 0; && \text{right of mpp} \end{aligned} \right\} \quad (14)$$

Since

$$\frac{dP_{pv}}{dv_{pv}} = \frac{d(v_{pv} * i_{pv})}{dv_{pv}} = i_{pv} + v_{pv} * \frac{di_{pv}}{dv_{pv}} \cong i_{pv} + v_{pv} * \frac{\Delta i_{pv}}{\Delta v_{pv}} \quad (15)$$

Therefore, (14) is rewritten as

$$\left. \begin{aligned} \frac{\Delta i_{pv}}{\Delta v_{pv}} &= -\frac{i_{pv}}{v_{pv}}; && \text{at mpp} \\ \frac{\Delta i_{pv}}{\Delta v_{pv}} &> -\frac{i_{pv}}{v_{pv}}; && \text{left of mpp} \\ \frac{\Delta i_{pv}}{\Delta v_{pv}} &< -\frac{i_{pv}}{v_{pv}}; && \text{right of mpp} \end{aligned} \right\} \quad (16)$$

Thus, based on the relation between INC and instantaneous conductance, the controller decides the direction of perturbation as shown in Fig. 3, and increases/decreases the duty cycle accordingly. For instance, on the right of MPP, the duty cycle is increased with a fixed perturbation size until the direction reverses. Ideally, the perturbation stops once the operating point reaches the MPP. However, in practice, operating point oscillates around the MPP.

As the perturbation size reduces, the controller takes more time to track the MPP of SPV array. An intellectual agreement between the tracking time and the perturbation size is held to fulfill the objectives of MPPT and soft starting of BLDC motor. In order to achieve soft starting, the initial value of duty cycle is set as zero. In addition, an optimum value of perturbation size ( $\Delta D=0.001$ ) is selected, which contributes to soft starting and also minimizes oscillations around the MPP.

## B. Electronic Commutation of BLDC Motor

The BLDC motor is controlled using a VSI operated through an electronic commutation of BLDC motor. An electronic commutation of BLDC motor stands for commutating the currents flowing through its windings in a predefined sequence using decoder logic. It symmetrically places the dc input current at the center of each phase voltage for  $120^\circ$ . Six switching pulses are generated as per the various possible combinations of three Hall-effect signals. These three Hall-effect signals are produced by an inbuilt encoder according to the rotor position.

A particular combination of Hall-effect signals is produced for each specific range of rotor position at an interval of  $60^\circ$  [5], [6]. The generation of six switching states with the estimation of rotor position is tabularized in Table II. It is perceptible that only two switches

conduct at a time, resulting in 120° conduction mode of operation of VSI and hence the reduced conduction losses. Besides this, the electronic commutation provides fundamental frequency switching of the VSI; hence, losses associated with high-frequency PWM switching are eliminated. A motor power company makes BLDC motor [28] with inbuilt encoder is selected for proposed system and its detailed specifications are given in the Appendixes.

## VI. CLOSED LOOP SPEED CONTROL OF BLDC MOTOR

In the sensed BLDC drive, hall sensors or a shaft encoder is used to obtain the rotor position information. The drive control system consists of an outer speed loop for speed control and an inner current loop for current control. Conventionally three separate current sensors are used to measure the phase currents. But here only one current sensor is used, which is placed on the DC link.

### A. Speed control

The speed control block uses a Proportional Integral (PI) controller. A PI controller attempts to correct the error between a measured process variable and desired set point by calculating and then outputting a corrective action that can adjust the process accordingly. The PI controller calculation involves two separate modes: the proportional mode and the integral mode. The proportional mode determines the reaction to the current error, integral mode determines the reaction based on recent error. The weighted sum of the two mode outputs as corrective action for the control element. The PI controller is widely used in the industry due to its ease in design and simple structure. The PI controller algorithm can be implemented as

$$output(t) = K_p e(t) + K_i \int_0^t e(\tau) d\tau \quad (17)$$

Here the input to speed controller is the speed error. The output of the controller is considered as a reference torque. A limit is put on the speed controller output depending on permissible maximum winding currents.

## VII. MATLAB/SIMULATION RESULTS

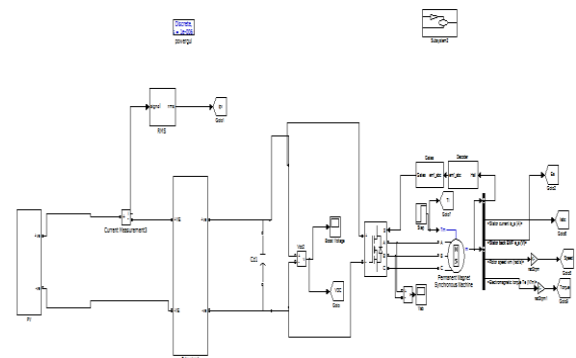
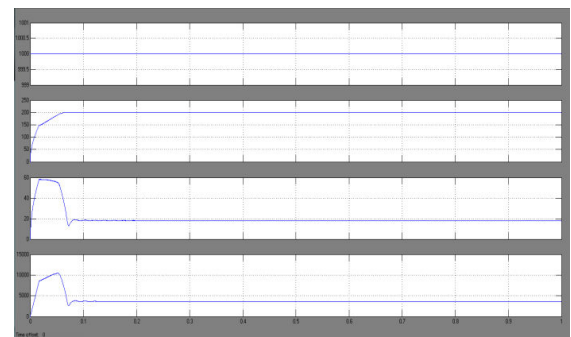
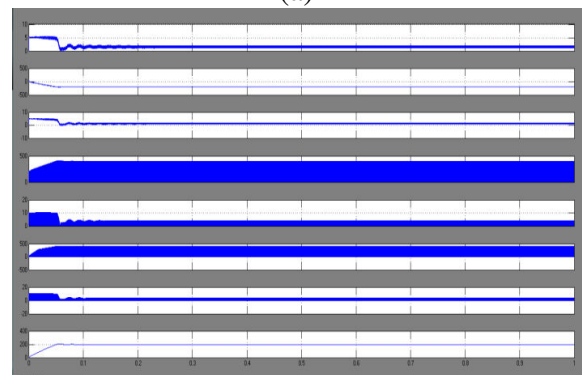


Fig. 4 Matlab/Simulink circuit of Starting and steady-state performances of the proposed SPV array-based zeta converter-fed BLDC motor drive for water pump

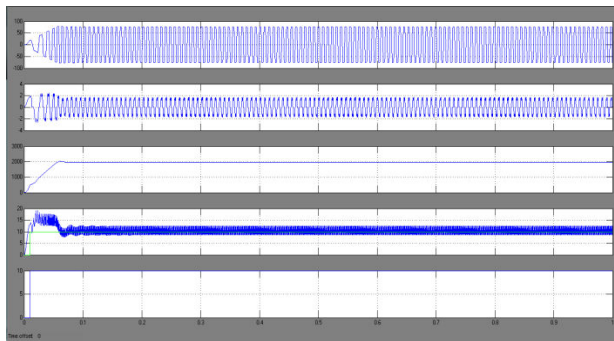


(a)



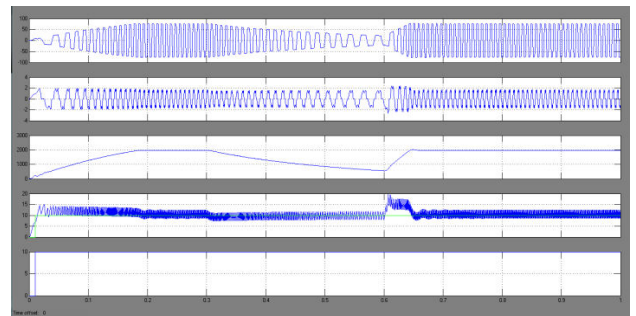
(b)





(c)

Fig.5 Starting and steady-state performances of the proposed SPV array-based zeta converter-fed BLDC motor drive for water pump. (a) SPV array variables. (b) Zeta converter variables. (c) BLDC motor-pump variables.



(c)

Fig.7 Dynamic performances of the proposed SPV array-based zeta converter-fed BLDC motor drive for water pump. (a) SPV array variables. (b) Zeta converter variables. (c) BLDC motor-pump variables.

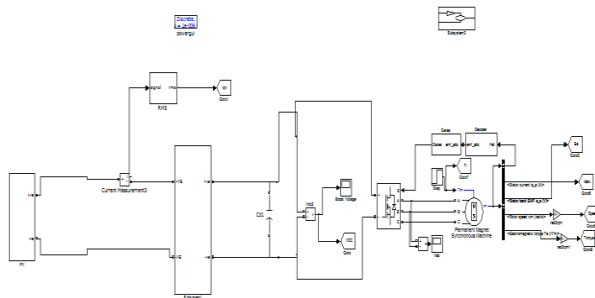


Fig.6 Matlab/Simulink circuit for Dynamic performance of SPV array-based zetaconverter-fed BLDC motor drive for water pump

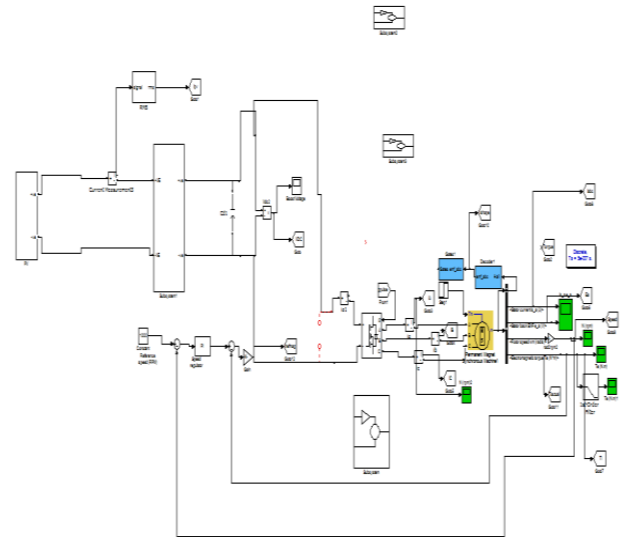
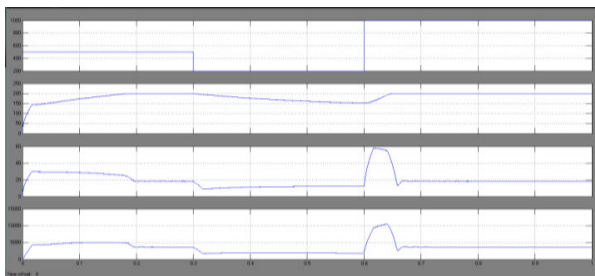
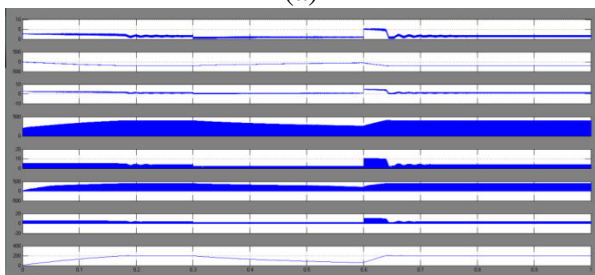


Fig.8 Matlab/Simulink circuit of SPV array-based zetaconverter-fed BLDC motor drive Closed loop control for water pumping system.



(a)



(b)

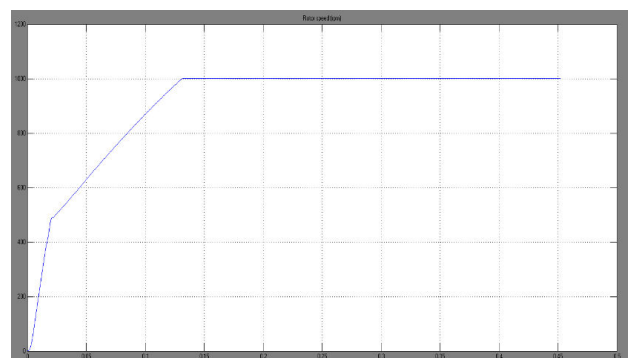


Fig.9 Speed.

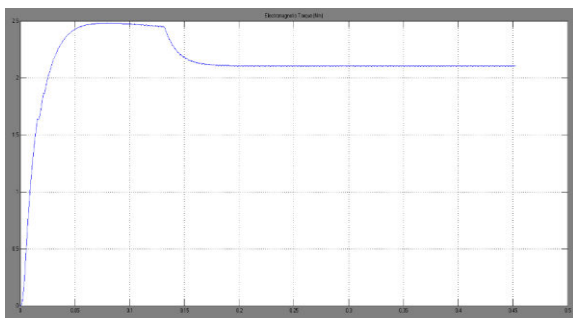


Fig.10 Torque.

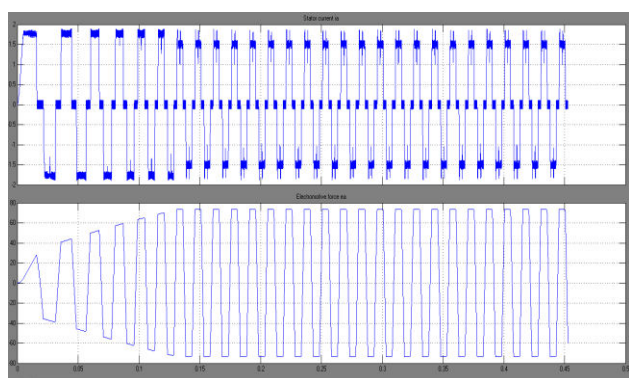


Fig.11 Stator current and emf.

## VIII CONCLUSION

A solar photovoltaic array fed Zeta converter based BLDC motor has been proposed to drive water-pumping system. The proposed system has been designed, modeled and simulated using MATLAB along with its Simulink and smpowersystemtoolboxes. Simulated results have demonstrated the suitability of proposed water pumping system. SPV array has been properly sized such that system performance is not influenced by the variation in atmospheric conditions and the associated losses and maximum switch utilization of Zeta converter is achieved. Zeta converter has been operated in CCM in order to reduce the stress on power devices. Operating the VSI in conduction mode with fundamental frequency switching eliminates the losses caused by high frequency switching operation. Stable operations of motor-pump system and safe

starting of BLDC motor are other important features of the proposed system.

## REFERENCES

- [1] M. Uno and A. Kukita, "Single-switch voltage equalizer using multistacked buck-boost converters for partially-shaded photovoltaic modules," *IEEE Trans. Power Electron.*, vol. 30, no. 6, pp. 3091–3105, Jun. 2015.
- [2] R. Arulmurugan and N. Suthanthiravanitha, "Model and design of a fuzzy-based Hopfield NN tracking controller for standalone PV applications," *Elect. Power Syst. Res.*, vol. 120, pp. 184–193, Mar. 2015.
- [3] S. Satapathy, K. M. Dash, and B. C. Babu, "Variable step size MPPT algorithm for photovoltaic array using zeta converter—A comparative analysis," in *Proc. Students Conf. Eng. Syst. (SCES)*, Apr. 12–14, 2013, pp. 1–6.
- [4] R. Kumar and B. Singh, "BLDC motor driven solar PV array fed waterpumping system employing zeta converter," in *Proc. 6th IEEE India Int. Conf. Power Electron. (IICPE)*, Dec. 8–10, 2014, pp. 1–6.
- [5] B. Singh, V. Bist, A. Chandra, and K. Al-Haddad, "Power factor correction in bridgeless-Luo converter-fed BLDC motor drive," *IEEE Trans. Ind. Appl.*, vol. 51, no. 2, pp. 1179–1188, Mar./Apr. 2015.
- [6] B. Singh and V. Bist, "Power quality improvements in a zeta converter for brushless dc motor drives," *IET Sci. Meas. Technol.*, vol. 9, no. 3, pp. 351–361, May 2015.
- [7] R. F. Coelho, W. M. dos Santos, and D. C. Martins, "Influence of power converters on PV maximum power point tracking efficiency,"



inProc.10th IEEE/IAS Int. Conf. Ind. Appl. (INDUSCON), Nov. 5–7, 2012, pp. 1–8.

[8] M. A. Elgendy, B. Zahawi, and D. J. Atkinson, “Assessment of the incremental conductance maximum power point tracking algorithm,” *IEEE Trans. Sustain. Energy*, vol. 4, no. 1, pp. 108–117, Jan. 2013.

[9] M. Sitbon, S. Schacham, and A. Kuperman, “Disturbance observer based voltage regulation of current-mode-boost-converter-interfaced photovoltaic generator,” *IEEE Trans. Ind. Electron.*, vol. 62, no. 9, pp. 5776–5785, Sep. 2015.

[10] R. Kumar and B. Singh, “Buck–boost converter fed BLDC motor drive for solar PV array based water pumping,” in *Proc. IEEE Int. Conf. Power Electron. Drives Energy Syst. (PEDES)*, Dec. 16–19, 2014, pp. 1–6.

[11] A. H. El Khateb, N. Abd. Rahim, J. Selvaraj, and B. W. Williams, “DC to dc converter with low input current ripple for maximum photovoltaic power extraction,” *IEEE Trans. Ind. Electron.*, vol. 62, no. 4, pp. 2246–2256, Apr. 2015.

[12] D. D. C. Lu and Q. N. Nguyen, “A photovoltaic panel emulator using a buck–boost dc/dc converter and a low cost micro-controller,” *Solar Energy*, vol. 86, no. 5, pp. 1477–1484, May 2012.

[13] Z. Xuesong, S. Daichun, M. Youjie, and C. Deshu, “The simulation and design for MPPT of PV system based on incremental conductance method,” in *Proc. WASE Int. Conf. Inf. Eng. (ICIE)*, Aug. 14–15, 2010, vol. 2, pp. 314–317.

[14] A. R. Reisi, M. H. Moradi, and S. Jamasb, “Classification and comparison of maximum power point tracking techniques for

photovoltaic system: A review,” *Renew. Sustain. Energy Rev.*, vol. 19, pp. 433–443, Mar. 2013.

[15] B. Bendib, H. Belmili, and F. Krim, “A survey of the most used MPPT methods: Conventional and advanced algorithms applied for photovoltaic systems,” *Renew. Sustain. Energy Rev.*, vol. 45, pp. 637–648, May 2015.